

Hydration Reaction Analysis of Calcium-Silicate-Based Materials using Scanning Electron Microscopy and X-Ray Diffraction Method

SUMMARY

Background/Aim: The components of calcium silicate-based materials can be identified through X-Ray Diffraction Analysis. This study aimed to determine the hydration reactions and particle size of MTA Angelus, Biodentine, and NeoMTA Plus as calcium-silicate-based materials. **Material and Methods:** The powder and set cement samples using divergence and scatter slits of 1° and a receiver slit of 0.10 mm. The scanning range was set at 5° to 70° , and ongoing scans for the theta-2theta range was performed with a scan speed of $2^\circ/\text{minute}$ (-1). The patterns obtained were analyzed using search-match software. The three most substantial peaks were used to identify hydration reactions and major crystalline structures. Also, Scanning Electron Microscope (SEM) analysis was performed and the particle size of set materials were determined using an image analysis software. **Results:** According to X-Ray Diffraction Analysis, the main components were determined as tricalcium silicate and dicalcium silicate in the three calcium silicate-based materials. We determined that the main components of the materials were similar. We also identified the extensive presence of tricalcium aluminate in MTA Angelus, calcium carbonate in Biodentine, and calcium phosphate salts in NeoMTA Plus. Furthermore, the results of the present particle analysis show that the calcium-silicate-based materials' distribution of particle count and size varies. Biodentine has the widest, and MTA Angelus has the narrowest particle size distribution range. NeoMTA Plus has the largest number of fine, large-sized particles ($p < 0.0001$), while MTA Angelus and Biodentine have a more homogeneous and non-statistically significant particle distribution range ($p > 0.05$). **Conclusions:** The present findings provide insight into variations in performance between different calcium-silicate-based materials.

Key words: Biodentine, MTA, NeoMTA, Scanning Electron Microscope, X-ray Diffraction

Abidin Talha Mutluay¹, Merve Mutluay¹, Adem Pehlivanli²

¹ Department of Dental Hygiene, Vocational School of Health Services, Kirikkale University, Kirikkale, Turkey

² Department of Medical Imaging, Vocational School of Health Services, Kirikkale University, Kirikkale, Turkey

ORIGINAL PAPER (OP)

Balk J Dent Med, 2022;133-141

Introduction

Mineral trioxide aggregate (MTA) is a biomaterial consisting of tricalcium silicate (53.1%), dicalcium silicate (22.5%), tricalcium oxide, and hydrophilic particles of silicate oxide.¹ Due to its biocompatibility and physicochemical characteristics, MTA has been used in pulp capping, pulpotomy, apexification, apexogenesis, perforation repairs, retrograde fillings, and orthograde canal fillings.² The calcium, phosphate, and hydroxyl

ions released during the MTA' setting reaction induce regeneration and remineralization of dental hard tissues.^{3,4}

Biodentine is a calcium-silicate-based material with a broad clinical application range similar to MTA.⁵ Biodentine powder mainly consists of tricalcium silicate and dicalcium silicate. Calcium carbonate has been added as a filler to improve its mechanical characteristics and zirconium dioxide to accelerate the setting reaction and provide radiopacity.⁶ Biodentine powder contains hydrosoluble polymers that reduce the water/powder ratio.⁷

NeoMTA Plus is another novel calcium silicate-based material with a wide application range obtained by mixing tricalcium silicate containing tantalum oxide (Ta_2O_5) with a water-based gel.⁸ It can be prepared with a fluid consistency for root canal filling or with a dense consistency for retrograde filling by adjusting its powder/gel ratio. The manufacturer states that this material can be used in vital pulp treatments (pulp capping, pulpotomy, or cavity lining/base), root apexification, root repairs (resorption or perforation), root tip filling, and root canal sealing.⁸

The X-ray diffraction (XRD) method is an analytic technique widely used to investigate and identify major crystalline structures.⁹ A substance either in pure form or as a mixture always produces a characteristic diffraction pattern. Due to this property, the content of any substance can be identified by comparing its diffraction pattern with a database or using a software.¹⁰ XRD enables the identification of the main components or compounds within a substance or mixture, which is essential for determining its physical, chemical, and mechanical properties. XRD is a reliable, precise, and reproducible method for measuring the relative phase abundances, physicochemical characteristics, and crystalline phases of materials.¹¹ The particle sizes of dental cements can affect their physical and biological properties and their setting time.^{12,13} Calcium-silicate-based materials can penetrate into dentinal tubules to provide effective sealing at the material-dentin interface owing to the fine-sized particles it contains.¹⁴

This study aimed to determine the hydration reactions and particle size of MTA Angelus, Biodentine, and NeoMTA Plus as calcium-silicate-based materials based on the null hypothesis that “there are no differences between the particle size and hydration reactions of calcium-silicate-based materials tested by X-ray diffractometry.”

Material and methods

The powder/liquid ratios of the different types of calcium-silicate-based cement were adjusted according to the manufacturers' instructions. After being placed on a clean, moisture-free glass plate, the powder and liquid were mixed manually using a metal cement spatula until the consistency of a homogenous paste was achieved. The mixed cement samples were squeezed into wax molds of 10 mm in diameter and 2 mm in height. The samples were kept in an incubator at 37°C and 100% humidity for 96 hours.

X-ray diffractometry (GNR, APD 2000 Pro, Italy) was performed on the powder and set cement samples using divergence and scatter slits of 1° and a receiver slit of 0.10 mm. The diffractometer was operated with a step size of 0.02° and an exposure time of 500 s at 45 kV and 40 mA. The samples' diffraction patterns were obtained at a scanning speed of 0.01°/min and $2\theta = 5\text{--}70.0^\circ$ using copper radiation ($\lambda[\text{CuK}\alpha] = 1.541874 \text{ \AA}$). Phase identification was performed on the obtained

patterns using search-match software (MATCH!-Phase Identification from Powder Diffraction Data, Crystal Impact, Germany, 2020). The three strongest peak points were used to identify the components of the different types of calcium silicate-based cement. The powder and set samples were also analyzed using a scanning electron microscope (SEM) (LEO 440, Leike Zeiss, K61n, Germany) at 1000× and 5000× magnification.

The particle sizes of the set samples were measured at 1000× magnification on the SEM images using ImageJ (National Institute of Health, Bethesda, Maryland, USA), an image analysis software. The data were analyzed using the statistical software package IBM SPSS Statistics 16.0. The particle sizes of calcium-silicate-based materials were compared using the Kruskal-Wallis and Mann-Whitney tests. A level of $p < 0.05$ was considered statistically significant.

Results

The XRD measurements of the MTA Angelus powder and set samples are shown in Figures 1a and 1b, respectively. The highest peak value of tricalcium silicate ($\text{Ca}_3[\text{SiO}_4]\text{O}$) was measured at $2\theta = 34.36^\circ$ in the powder sample and at $2\theta = 32.79^\circ$ in the set sample. Regarding dicalcium silicate ($\text{Ca}_2[\text{SiO}_4]$), the highest peak value was measured at $2\theta = 32.11^\circ$ in the powder sample and $2\theta = 32.01^\circ$ in the set sample. Other components had their highest peak values in the powder and set samples at the following values, respectively: $2\theta = 33.29^\circ$ and $2\theta = 33.19^\circ$ for tricalcium aluminate ($\text{Ca}_3\text{Al}_2\text{O}_6$), $2\theta = 29.08^\circ$ and $2\theta = 29.22^\circ$ for calcium carbonate (CaCO_3), $2\theta = 34.22^\circ$ and $2\theta = 36.07^\circ$ for calcium hydroxide ($\text{Ca}[\text{OH}]_2$), $2\theta = 45.77^\circ$ and $2\theta = 45.95^\circ$ for aluminum oxide (Al_2O_3), and $2\theta = 28.23^\circ$ and $2\theta = 27.88^\circ$ for bismuth oxide (Bi_2O_3). Calcium tungstate (CaWO_4) was identified in the powder sample but not in the set sample, with its highest peak value found at $2\theta = 28.76^\circ$. On the other hand, calcium phosphate ($\text{Ca}_3[\text{PO}_4]_2$) was identified in the set sample but not in the powder sample, with its highest peak value at $2\theta = 25.40^\circ$.

The XRD measurements of the Biodentine powder and set samples are shown in Figures 1c and 1d, respectively. The highest peak of tricalcium silicate ($\text{Ca}_3[\text{SiO}_4]\text{O}$) was measured at $2\theta = 32.22^\circ$ in the powder sample and at $2\theta = 33.18^\circ$ in the set sample. Regarding dicalcium silicate ($\text{Ca}_2[\text{SiO}_4]$), the highest peak value was measured at $2\theta = 32.23^\circ$ in the powder sample and at $2\theta = 31.90^\circ$ in the set sample. The peak values for other components in the powder and set samples were, respectively, $2\theta = 29.51^\circ$ and $2\theta = 29.80^\circ$ for calcium carbonate (CaCO_3), $2\theta = 29.14^\circ$ and $2\theta = 29.39^\circ$ for calcium chloride (CaCl_2), $2\theta = 28.12^\circ$ and $2\theta = 30.15^\circ$ for zirconium oxide (ZrO_2), $2\theta = 34.05^\circ$ and $2\theta = 36.41^\circ$ for calcium hydroxide ($\text{Ca}[\text{OH}]_2$), and $2\theta = 37.90^\circ$ and $2\theta = 37.61^\circ$ for calcium oxide (CaO).

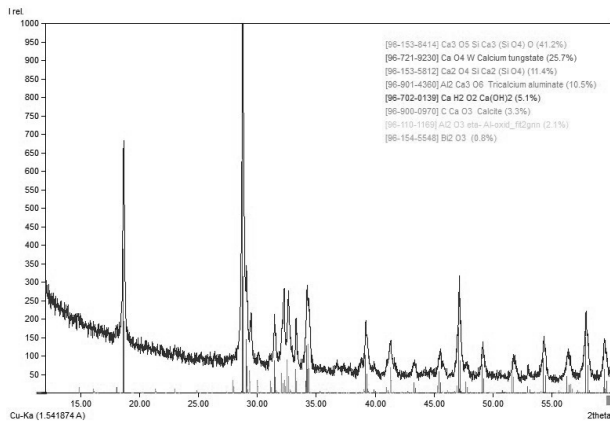


Figure 1a. X-ray diffraction analysis of MTA Angelus powder sample. The three strongest peak points were used to identify the components of the material.

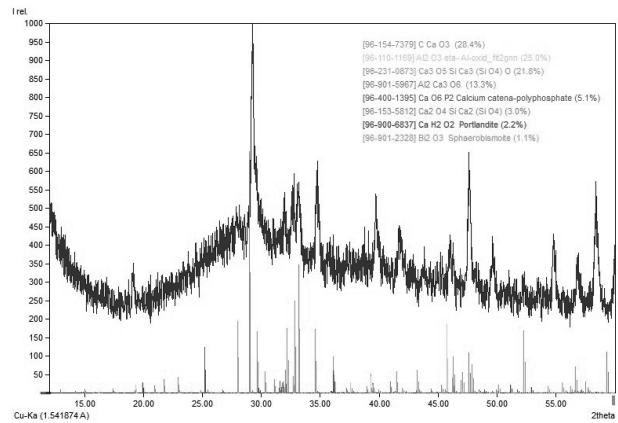


Figure 1b. X-ray diffraction analysis of MTA Angelus set sample. The three strongest peak points were used to identify the components of the material.

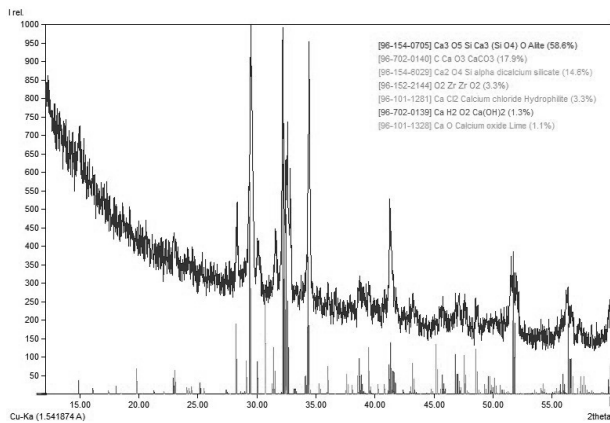


Figure 1c. X-ray diffraction analysis of Biodentine powder sample. The three strongest peak points were used to identify the components of the material.

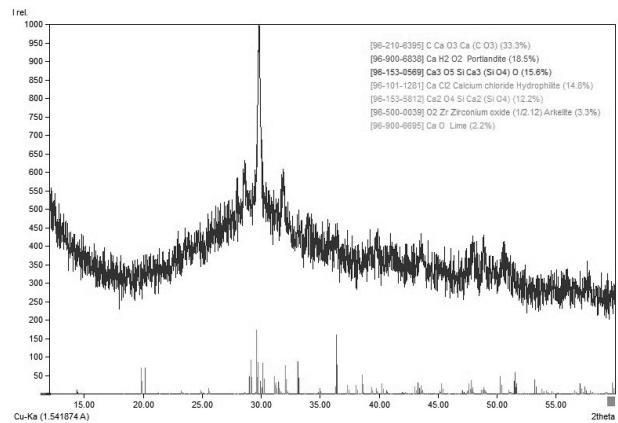


Figure 1d. X-ray diffraction analysis of Biodentine set sample. The three strongest peak points were used to identify the components of the material.

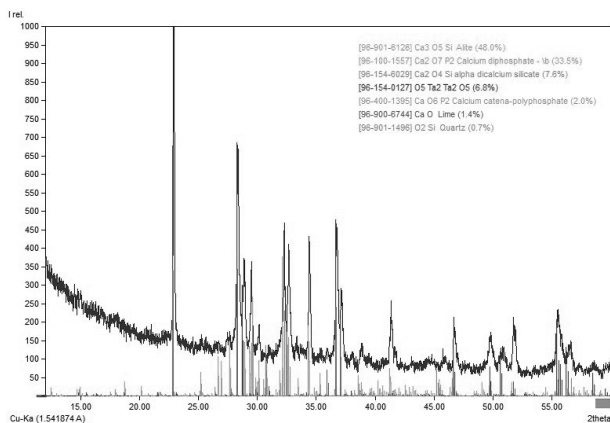


Figure 1e. X-ray diffraction analysis of NeoMTA Plus powder sample. The three strongest peak points were used to identify the components of the material.

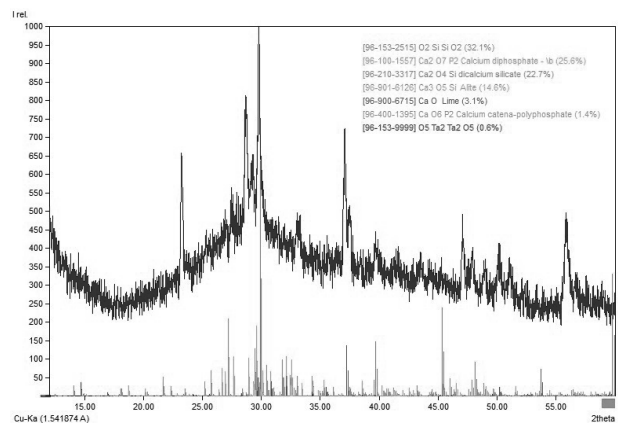


Figure 1f. X-ray diffraction analysis of NeoMTA Plus set sample. The three strongest peak points were used to identify the components of the material.

XRD measurements are shown in Figure 1e for the NeoMTA Plus powder sample and Figure 1f for the set sample. The highest peak values of the components in the powder and set samples were, respectively, as follows: $2\theta=32.29^\circ$ and $2\theta=31.99^\circ$ for tricalcium silicate ($\text{Ca}_3(\text{SiO}_4)\text{O}$), $2\theta=32.29^\circ$ and $2\theta=27.11^\circ$ for dicalcium

silicate ($\text{Ca}_2(\text{SiO}_4)$), $2\theta=29.50^\circ$ and $2\theta=29.61^\circ$ for calcium pyrophosphate ($\text{Ca}_2\text{P}_2\text{O}_7$), $2\theta=25.24^\circ$ and $2\theta=25.33^\circ$ for calcium metaphosphate ($\text{Ca}(\text{PO}_3)_2$), $2\theta=28.34^\circ$ and $2\theta=29.61^\circ$ for tantalum oxide (Ta_2O_5), $2\theta=27.94^\circ$ and $2\theta=29.79^\circ$ for silicium oxide (SiO_2), and $2\theta=35.96^\circ$ and $2\theta=37.41^\circ$ for calcium oxide (CaO).

SEM micrographs of the powder and set samples of three materials at 1000 \times and 5000 \times magnification are displayed in Figures 2a–c and 3a–c. Irregular particles with different shapes and sizes were observed in the MTA Angelus powder samples. In addition to flat-surfaced and angular particles, small, round, and/or popcorn-like particles were also observed. The particle samples of the Biodentine powder were observed to have nested structures. They had either a round or oval appearance, and like the MTA Angelus particles, varied in size. The NeoMTA Plus powder samples consisted of interconnected particles of different sizes, and the particles had an angular, flat-surfaced, or globular appearance.

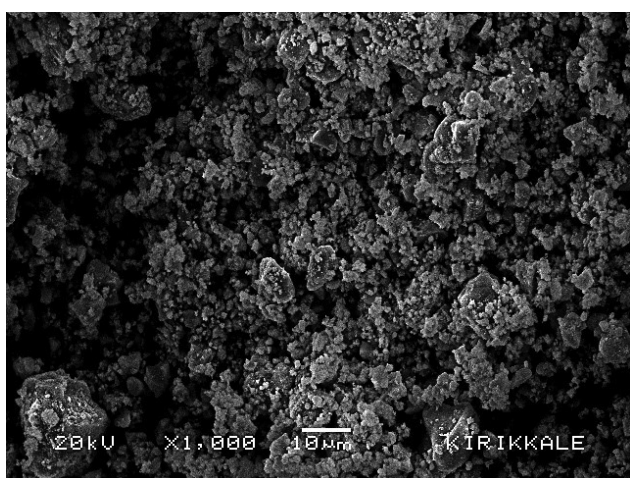


Figure 2a. SEM images of the powder samples of MTA Angelus at 1000 \times magnification. Irregular particles with different shapes and sizes were observed in the MTA Angelus powder samples.

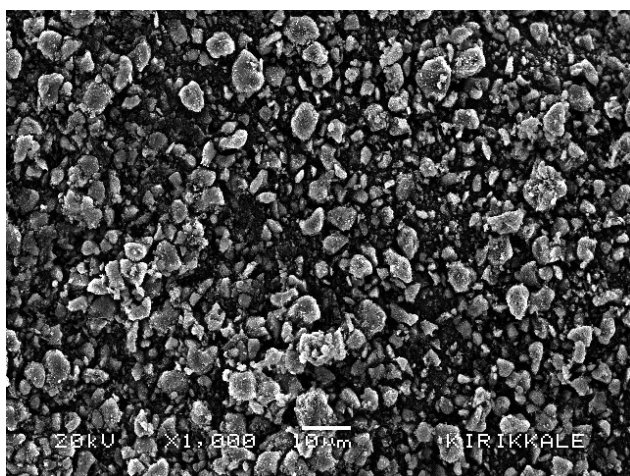


Figure 2b. SEM images of the powder samples of Biodentine at 1000 \times magnification. The particle samples of the Biodentine powder were observed to have nested structures

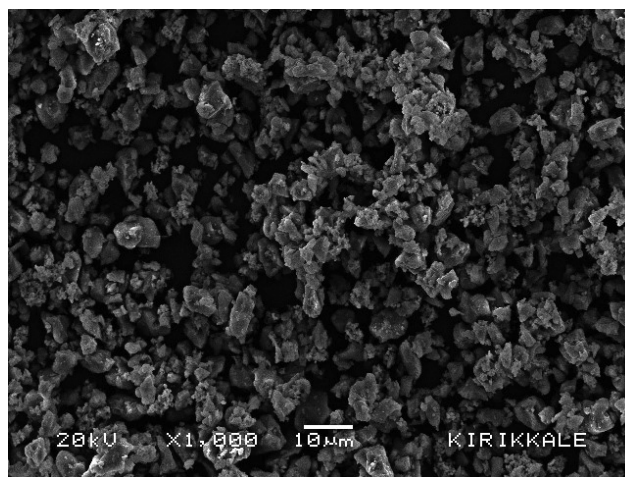


Figure 2c. SEM images of the powder samples of NeoMTA Plus at 1000 \times magnification. The NeoMTA Plus powder samples consisted of interconnected particles of different sizes, and the particles had an angular, flat-surfaced, or globular appearance.

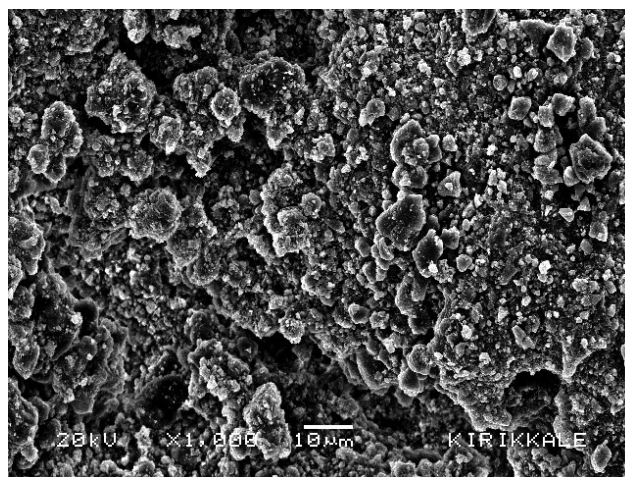


Figure 3a. SEM images of the set samples of MTA Angelus at 1000 \times magnification. All three materials showed a dissimilar particle count and size distribution on set samples.

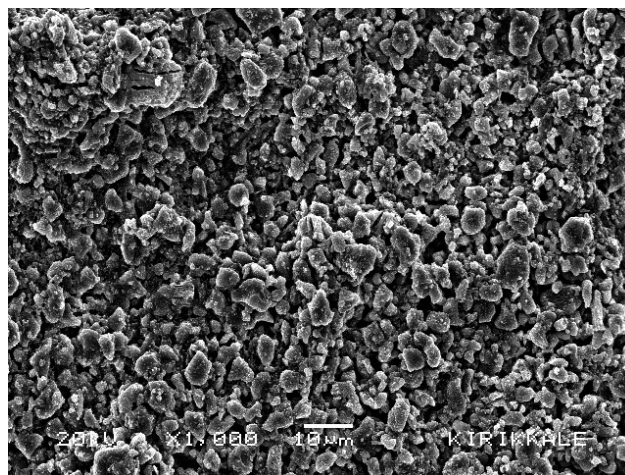


Figure 3b. SEM images of the set samples of Biodentine at 1000 \times magnification. All three materials showed a dissimilar particle count and size distribution on set samples.

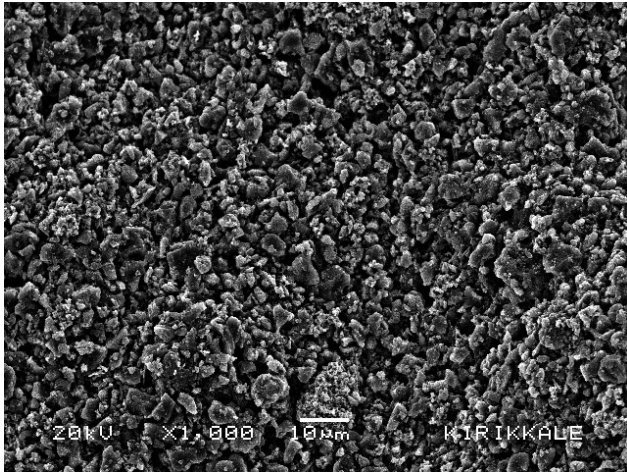


Figure 3c. SEM images of the set samples of NeoMTA Plus at 1000x magnification. All three materials showed a dissimilar particle count and size distribution on set samples.

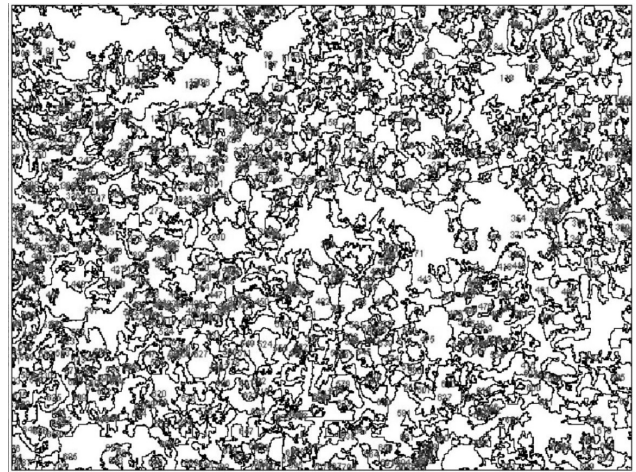


Figure 4b. Drawing of Biodentine set sample for particle size assessment using image analysis software (ImageJ). The mean particle size of material was calculated to be min-max: 0.22-49.46 μm .

All three materials showed a dissimilar particle count and size distribution (Figure 4a-c). The mean particle number of each material was calculated to be 882 for MTA Angelus, 692 for Biodentine, and 973 for NeoMTA Plus. Particle size ranged more widely for Biodentine (min-max: 0.22-49.46 μm) and NeoMTA Plus (min-max: 0.21-47.69 μm) than for MTA Angelus (min-max: 0.22-46.15 μm). While MTA Angelus (2.30 μm) was observed to have a lower mean particle size compared to Biodentine (2.66 μm), the difference was not significant ($p > 0.05$). However, the mean particle size of NeoMTA Plus (3.28 μm) is significantly higher than that of both Biodentine and MTA Angelus ($p < 0.0001$).

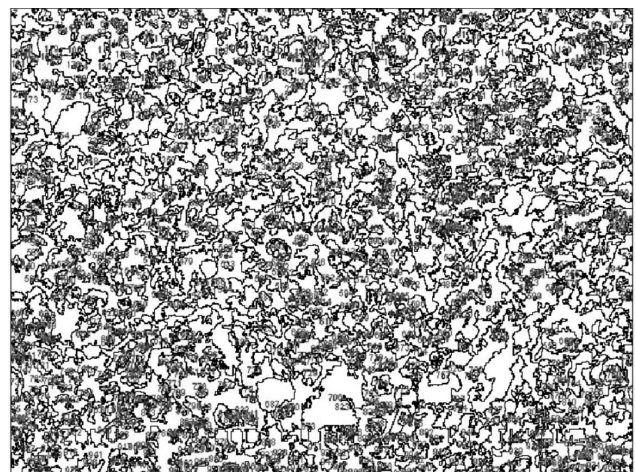


Figure 4c. Drawing of NeoMTA Plus set sample for particle size assessment using image analysis software (ImageJ). The mean particle size of material was calculated to be min-max: 0.21-47.69 μm .

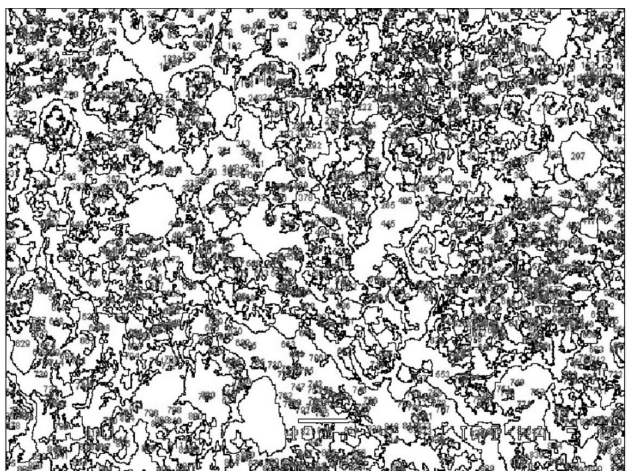


Figure 4a. Drawing of MTA Angelus set sample for particle size assessment using image analysis software (ImageJ). The mean particle size of material was calculated to be min-max: 0.22-46.15 μm .

Discussion

X-ray diffraction (XRD) is an analytic method that enables the identification of the crystallographic characteristics and phases of materials. The XRD method is based on the principle that each crystal diffracts X-rays in a characteristic order related to the specific atomic sequence of its phase. Thus, the crystalline structure, phases, and particle size of a sample can be identified by directing X-rays into it. Additional information about the sample's phases can be determined by comparing the data obtained from the X-ray to a related database of samples with unidentified phases. Diffraction profiles in such databases provide crystal information for each

crystalline phase. X-ray diffraction peaks are created by the interaction of monochromatic X-ray beams scattered by a sample at specific angles. The peak densities are determined according to the distribution of atoms within the crystalline structure. In other words, the X-ray diffraction model is the fingerprint of the periodic atomic sequence in a particular material¹⁵.

The components of calcium silicate-based dental materials can be identified through XRD analysis. The principle component and most reactive of these materials is tricalcium silicate, which has high biocompatibility and bioactivity^{1,16,17}. Tricalcium silicate reacts with tissue fluids to induce hydroxyapatite formation through the creation of calcium silicate hydrate and calcium hydroxide¹⁶. Also, tricalcium silicate, which is a biocompatible content, induces the differentiation of human dental pulp cells¹⁸. With the presence of calcium chloride and tricalcium silicate, the setting reaction is accelerated and bioactivity/biocompatibility are improved¹⁹.

In this study, we used XRD analysis to investigate hydration reactions and crystalline phases of MTA Angelus, Biodentine, and NeoMTA Plus, which are calcium silicate-based materials. We determined that the main components of the materials were similar. We also identified the extensive presence of tricalcium aluminate in MTA Angelus, calcium carbonate in Biodentine, and calcium phosphate salts in NeoMTA Plus.

According to the literature, the essential components of MTA Angelus are tricalcium silicate, dicalcium silicate, and tricalcium aluminate. In addition to these components, calcium oxide, aluminum oxide, and silicium oxide are also present. Tricalcium aluminate, which is considered one of the main phases of MTA Angelus, is among the most reactive components and reacts very rapidly with water; however, its contribution to physical endurance is minimal¹⁹. In a study that called the literature into question, Islam et al. used XRD analysis to show that MTA's essential components are tricalcium silicate, tricalcium aluminate, calcium silicate, tetracalcium aluminoferrite, and bismuth oxide⁹. In their XRD analysis, Lee et al.²⁰ observed several sharp peaks of tricalcium silicate, tricalcium aluminate, and calcium silicate in unhydrated MTA. Furthermore, they reported that tricalcium silicate, calcium silicate, and tricalcium aluminate phases were observed but with decreased linear densities in hydrated samples.

Contrary to the findings of Lee et al.²⁰, our study showed that the components with firm peaks of the MTA Angelus powder sample were tricalcium silicate ($2\theta=34.36^\circ$), calcium tungstate ($2\theta=28.76^\circ$), dicalcium silicate ($2\theta=32.11^\circ$), and tricalcium aluminate ($2\theta=33.29^\circ$). We observed that in set samples of tricalcium silicate and dicalcium silicate, their densities ($2\theta=32.79^\circ$ and $2\theta=32.01^\circ$, respectively) decreased

at peak values compared to baseline measurements. However, the densities of calcium carbonate ($2\theta=29.22^\circ$) and calcium phosphate ($2\theta=25.40^\circ$) at peak values increased. Following the setting reaction, we could not identify calcium tungstate ($2\theta=28.76^\circ$) in the powder sample. Calcium tungstate is known to be a radiopacifier, so our inability to detect it shows that this component might be a reactant in the setting reaction. Therefore calcium tungstate, might have contributed to the formation of other components and/or their increased densities.

The principal component of Biodentine is tricalcium silicate⁶, and Biodentine powder includes refined grains of calcium silicate and calcium chloride (CaCl_2). The liquid form of CaCl_2 serves both as an accelerator for tricalcium silicate and a water-soluble polymer⁷. Calcium carbonate, present in Biodentine, serves as a nucleation site for carbon-sulfur-hydrogen and reduces the induction period. In our study, we considered that an increase in Biodentine's mechanical endurance occurs following the rapid peak observed after 30 minutes⁶. We identified tricalcium silicate ($2\theta=32.22^\circ$) and dicalcium silicate ($2\theta=32.23^\circ$) in the Biodentine samples. Moreover, we determined that the densities of the tricalcium silicate ($2\theta=33.18^\circ$) and dicalcium silicate ($2\theta=31.90^\circ$) decreased after the setting reaction, whereas the density of the calcium carbonate ($2\theta=29.80^\circ$) increased. In their XRD analysis, Camilleri et al.⁶ reported that tricalcium silicate, calcium carbonate, and zirconium oxide were identified, but unlike in our study, dicalcium silicate was not.

NeoMTA Plus, a novel calcium silicate-based material, was introduced as a rapidly setting root repair material that, due to the presence of gel within its liquid, has optimal consistency, is easily manipulated, and does not cause any coloration^{21,22}. However, little information about NeoMTA Plus is available in the literature, and its hydration reaction is not yet fully understood. In the XRD analysis performed by Abu Zeid et al.²³, calcium silicate, calcium phosphate, calcium aluminum oxide, and calcium sulfate were determined to be present in NeoMTA Plus. In the energy dispersive X-Ray (EDX) analysis conducted in the same study, NeoMTA Plus was determined to have a higher sulfur and aluminum content than MTA Angelus, and these elements were reported to be possibly related to the more rapid setting of NeoMTA Plus. In addition, it was reported that NeoMTA Plus could be used as an alternative to MTA Angelus because of its higher crystallinity and better bioactivity. On the other hand, in our study, we identified tricalcium silicate ($2\theta = 32.29^\circ$; $2\theta = 31.99^\circ$), dicalcium silicate ($2\theta = 32.29^\circ$; $2\theta = 27.11^\circ$), calcium phosphate pyrophosphate ($2\theta = 29.50^\circ$; $2\theta = 29.61^\circ$), calcium metaphosphate ($2\theta = 25.24^\circ$; $2\theta = 25.33^\circ$), tantalum oxide ($2\theta = 28.34^\circ$; $2\theta = 29.61^\circ$), silicium oxide ($2\theta = 27.94^\circ$), and calcium oxide ($2\theta = 35.96^\circ$, $2\theta = 37.41^\circ$) in the content of NeoMTA

Plus. Contrary to the abovementioned study, in our study, we identified no sulfur or aluminum in their pure forms and determined that these components were involved in the structure of various compounds.

Whether calcium oxide is present in calcium silicate-based materials and how it is formed is not identified in the current literature. One study reported that calcium hydroxide was released during the setting reaction due to calcium oxide's very rapid hydration following an intense exothermic reaction. In addition, calcium hydroxide was reported to be produced as a by-product of the reaction and was intensely released in MTA Angelus due to calcium oxide's hydration⁶. On the contrary, Camilleri *et al.*²⁴ reported that all tricalcium silicate-based materials did not necessarily produce calcium hydroxide after the hydration reaction. Even though the reaction product was free calcium hydroxide, various ingredients might have reacted with it, and thus, its amount might have decreased. According to Abu Zeid *et al.*²³, the fact that calcium hydroxide was not present in set samples revealed that this component had participated in the setting reaction. On the other hand, in our study, calcium oxide was identified in Biodentine and NeoMTA Plus in the XRD analysis of powder and set samples. Calcium hydroxide was determined to be present at similar levels in the powder and set MTA Angelus samples, whereas it was present at an exceptionally high level in the set Biodentine sample and could not be identified in the powder and set samples of NeoMTA Plus. This result is consistent with previous studies showing that calcium oxide and calcium hydroxide participated in hydration reactions²³⁻²⁵.

As radiopacifying phases, Biodentine involves zirconium oxide, MTA Angelus involves bismuth oxide, and NeoMTA Plus involves tantalum oxide²⁶. Bismuth oxide, present as a radiopacifier in powder MTA, also plays a significant role in cement hydration. Bismuth oxide was reported to cause coloration of tooth tissues, reduced calcium hydroxide release, increased solubility, and thus, deterioration of the material's structure²⁷. Moreover, bismuth oxide significantly increased the setting period and reduced the cement's compressive endurance¹; additionally, it was shown to interfere with cellular growth²⁸. Such adverse features affect the material's biocompatibility²⁹, and it has been recommended that bismuth oxide be replaced by an alternative radiopacifying ingredient³⁰. In this regard, tantalum oxide was added as a radiopacifying agent, and NeoMTA Plus, a calcium silicate-based material, was developed. It has been reported that tantalum oxide was biocompatible with calcium phosphate-based materials that can replace the bone³¹, and due to its low toxicity and radiopacity, could be used as a scaffold for restorative treatments³². Zirconium oxide, another alternative radiopacifying component, has been added to Biodentine.

Using zirconium oxide has provided sufficient radiopacity and stability without the risk of discoloration, which has been associated with all materials using bismuth oxide as a radiopacifier^{7,33}. In our study, similar to previous studies, the presence of bismuth oxide in MTA Angelus samples^{1,6,23}, zirconium oxide in Biodentine²⁴, and tantalum oxide in NeoMTA Plus²³ were confirmed as radiopacifier ingredients.

The conventional method of quantifying a phase within a composite compares the peak height and peak area¹⁰. However, when a comparative analysis is made on Powder Diffraction Files (PDF), various challenges, including errors in an unknown diffraction model, overlapping peaks, and PDF errors, are encountered. Additionally, the absolute amounts of the peaks cannot be determined in the presence of overlapping peaks⁹. In their study in which they performed a manual match-analysis on PDF without using any software, Abu Zeid *et al.*²³ claimed that zirconium oxide was used as a radiopacifier, and no other radiopacifying agent was present in MTA Angelus. Similar to previous studies using search-match software^{1,6,20}, bismuth oxide was identified as a radiopacifying agent in our study's MTA Angelus powder sample. Moreover, unlike previous studies, we identified calcium tungstate in the powder sample of MTA Angelus. Analysis with search-match software might be an effective method to meticulously investigate the material's content.

The particle size of cements is fundamental to regarding the cement's setting reactions, biological and physical properties, and the extent of penetration into dentin tubules¹²⁻¹⁴. The results of the present particle analysis show that the calcium-silicate-based materials' distribution of particle count and size varies. Biodentine has the widest, and MTA Angelus has the narrowest particle size distribution range. NeoMTA Plus has the largest number of fine, large-sized particles ($p < 0.0001$), while MTA Angelus and Biodentine have a more homogeneous and non-statistically significant particle distribution range ($p > 0.05$). The present findings provide insight into variations in performance between different calcium-silicate-based materials¹⁴.

Conclusions

The main components of the materials were similar. We also identified the extensive presence of tricalcium aluminate in MTA Angelus, calcium carbonate in Biodentine, and calcium phosphate salts in NeoMTA Plus. Furthermore, The results of the present particle analysis show that the calcium-silicate-based materials' distribution of particle count and size varies. The present findings provide insight into variations in performance between different calcium-silicate-based materials.

References

- Camilleri J. Characterization of hydration products of mineral trioxide aggregate. *Int Endod J*, 2008;41:408-417.
- Torabinejad M, Parirokh M. Mineral trioxide aggregate: a comprehensive literature review--part II: leakage and biocompatibility investigations. *J Endod*, 2010;36:190-202.
- Martin RL, Monticelli F, Brackett WW, Loushine RJ, Rockman RA, Ferrari M, et al. Sealing properties of mineral trioxide aggregate orthograde apical plugs and root fillings in an in vitro apexification model. *J Endod*, 2007;33:272-275.
- Gandolfi MG, Parrilli AP, Fini M, Prati C, Dummer PM. 3D micro-CT analysis of the interface voids associated with Thermafil root fillings used with AH Plus or a flowable MTA sealer. *Int Endod J*, 2013;46:253-263.
- Nowicka A, Lipski M, Parafiniuk M, Sporniak-Tutak K, Lichota D, Kosierkiewicz A, et al. Response of human dental pulp capped with biodentine and mineral trioxide aggregate. *J Endod*, 2013;39:743-747.
- Camilleri J, Sorrentino F, Damidot D. Investigation of the hydration and bioactivity of radiopacified tricalcium silicate cement, Biodentine and MTA Angelus. *Dent Mater*, 2013;29:580-593.
- Camilleri J. Biodentine™ : the dentine in a capsule or more? : Septodont; 2018 [Available from: <https://www.septodontcorp.com/wp-content/uploads/2018/02/Biodentine-Article-0118-LOW.pdf>. Access 17 Sep, 2020.
- Avalon-Biomed. NeoMTAPlus Directions for use 2017 [Available from: <https://www.avalonbiomed.com/wp-content/uploads/2014/04/DFUNeoMTA-%20Plus-REV-1601.pdf>. Access 21 May, 2020.
- Islam I, Chng HK, Yap AU. X-ray diffraction analysis of mineral trioxide aggregate and Portland cement. *Int Endod J*, 2006;39:220-225.
- Cullity BD, Stock SR. *Elements of X-ray Diffraction*. 3rd ed. London: Prentice-Hall International; 2001.
- Walenta G, Füllmann T. Advances in quantitative XRD analysis for clinker, cements, and cementitious additions. *Powder Diffraction*, 2004;19:40-44.
- Komabayashi T, Spangberg LS. Comparative analysis of the particle size and shape of commercially available mineral trioxide aggregates and Portland cement: a study with a flow particle image analyzer. *J Endod*, 2008;34:94-98.
- Torabinejad M, Moazzami SM, Moaddel H, Hawkins J, Gustafson C, Faras H, et al. Effect of MTA particle size on periapical healing. *Int Endod J*, 2017;50 Suppl 2:e3-e8.
- Ha WN, Shakibaie F, Kahler B, Walsh LJ. Deconvolution of the particle size distribution of ProRoot MTA and MTA Angelus. *Acta Biomater Odontol Scand*, 2016;2:7-11.
- Bunaciu AA, Udriștioiu EG, Aboul-Enein HY. X-ray diffraction: instrumentation and applications. *Crit Rev Anal Chem*, 2015;45:289-299.
- Camilleri J. Characterization and hydration kinetics of tricalcium silicate cement for use as a dental biomaterial. *Dent Mater*, 2011;27:836-844.
- Belio-Reyes IA, Bucio L, Cruz-Chavez E. Phase composition of ProRoot mineral trioxide aggregate by X-ray powder diffraction. *J Endod*, 2009;35:875-878.
- Peng W, Liu W, Zhai W, Jiang L, Li L, Chang J, et al. Effect of tricalcium silicate on the proliferation and odontogenic differentiation of human dental pulp cells. *J Endod*, 2011;37:1240-1246.
- Wang X, Sun H, Chang J. Characterization of Ca3SiO5/CaCl2 composite cement for dental application. *Dent Mater*, 2008;24:74-82.
- Lee YL, Lee BS, Lin FH, Yun Lin A, Lan WH, Lin CP. Effects of physiological environments on the hydration behavior of mineral trioxide aggregate. *Biomaterials*, 2004;25:787-793.
- Türker SA, Uzunoğlu E, Bilgin B. Comparative evaluation of push-out bond strength of Neo MTA Plus with Biodentine and white ProRoot MTA. *J Adhes Sci Technol*, 2017;31:502-508.
- Camilleri J. Staining Potential of Neo MTA Plus, MTA Plus, and Biodentine Used for Pulpotomy Procedures. *J Endod*, 2015;41:1139-1145.
- Abu Zeid ST, Alamoudi NM, Khafagi MG, Abou Neel EA. Chemistry and Bioactivity of NeoMTA Plus™ versus MTA Angelus® Root Repair Materials. *J Spectrosc*, 2017;2017:1-9.
- Camilleri J. Hydration characteristics of Biodentine and Theracal used as pulp capping materials. *Dent Mater*, 2014;30:709-715.
- Camilleri J, Sorrentino F, Damidot D. Characterization of un-hydrated and hydrated BioAggregate™ and MTA Angelus™. *Clin Oral Investig*, 2015;19:689-698.
- Tomas-Catala CJ, Collado-Gonzalez M, Garcia-Bernal D, Onate-Sanchez RE, Forner L, Lena C, et al. Comparative analysis of the biological effects of the endodontic bioactive cements MTA-Angelus, MTA Repair HP and NeoMTA Plus on human dental pulp stem cells. *Int Endod J*, 2017;50 Suppl 2:e63-e72.
- Camilleri J. Evaluation of the effect of intrinsic material properties and ambient conditions on the dimensional stability of white mineral trioxide aggregate and Portland cement. *J Endod*, 2011;37:239-245.
- Camilleri J, Montesin FE, Papaioannou S, McDonald F, Pitt Ford TR. Biocompatibility of two commercial forms of mineral trioxide aggregate. *Int Endod J*, 2004;37:699-704.
- Gandolfi MG, Ciapetti G, Taddei P, Perut F, Tinti A, Cardoso MV, et al. Apatite formation on bioactive calcium-silicate cements for dentistry affects surface topography and human marrow stromal cells proliferation. *Dent Mater*, 2010;26:974-992.
- Camilleri J, Gandolfi MG. Evaluation of the radiopacity of calcium silicate cements containing different radiopacifiers. *Int Endod J*, 2010;43:21-30.
- Hoekstra JWM, van den Beucken JJ, Leeuwenburgh SC, Bronkhorst EM, Meijer GJ, Jansen JA. Tantalum oxide and barium sulfate as radiopacifiers in injectable calcium phosphate-poly (lactic-co-glycolic acid) cements for monitoring in vivo degradation. *J Biomed Mater Res Part A*, 2014;102:141-149.
- Mohandas G, Oskolkov N, McMahon MT, Walczak P, Janowski M. Porous tantalum and tantalum oxide nanoparticles for regenerative medicine. *Acta Neurobiol Exp (Wars)*, 2014;74:188-196.

33. Marciano MA, Duarte MA, Camilleri J. Dental discoloration caused by bismuth oxide in MTA in the presence of sodium hypochlorite. Clin Oral Investig, 2015;19:2201-2209.

Received on November 29, 2021.

Revised on January 12, 2022.

Accepted on March 24, 2022.

Conflict of Interest: Nothing to declare

Financial Disclosure Statement: Nothing to declare

Human Rights Statement: None required.

Animal Rights Statement: None required.

Correspondence

Merve Mutluay

Department of Dental Hygiene

Kirikkale University, Vocational School of Health Services

Kirikkale, Turkey

e-mail: m.mutluay@kku.edu.tr